


Suppression effect on the Berezinskii-Kosterlitz-Thouless transition in growing networks

S. M. Oh,¹ S.-W. Son,^{2,3,*} and B. Kahng^{1,†}¹CCSS, CTP and Department of Physics and Astronomy, Seoul National University, Seoul 08826, Korea²Department of Applied Physics, Hanyang University, Ansan 15588, Korea³Asia Pacific Center for Theoretical Physics, Pohang 37673, Korea (Received 21 March 2018; revised manuscript received 10 September 2018; published 7 December 2018)

The percolation transition in growing networks can be of infinite order, following the Berezinskii-Kosterlitz-Thouless (BKT) transition. Examples can be found in diverse systems, including coauthorship networks and protein interaction networks. Here, we investigate how such an infinite-order percolation transition is changed by the global suppression (GS) effect. We find that the BKT infinite-order transition breaks down, but the features of infinite-order, second-order, and first-order transitions all emerge in a single framework. Owing to the GS effect, the transition point p_c is delayed, below which the critical region is extended. The power-law behavior of the cluster size distribution reaches the state with the exponent $\tau = 2$ at p_c , suggesting that the system has the maximum diversity of cluster sizes and a first-order percolation transition occurs at p_c .

DOI: [10.1103/PhysRevE.98.060301](https://doi.org/10.1103/PhysRevE.98.060301)

Since the discovery a half century ago [1] that $1/r^2$ -type long-range interactions in the one-dimensional Ising model change the phase transition type, a subject associated with long-range interactions in diverse equilibrium and nonequilibrium systems has received considerable attention. In percolation, $1/r^2$ -type long-range connections in Euclidean space change the transition type to an infinite-order transition [2]. However, the idea of long-range connections cannot be implemented on complex networks. Hence, modeling a first-order percolation transition (PT) in random graphs has been a challenging task. Against this background, an explosive percolation model was introduced [3], in which clusters grow according to the so-called power-of-choice rule. Two merging clusters are optimally selected from multiple candidates to form a giant cluster that emerges abruptly. However, it was revealed that a *global suppression* (GS) rule is necessary to guarantee a first-order PT [4]. In fact, several cluster merging models that exhibit first-order PTs contain the key factor of GS. Those models include the spanning-cluster-avoiding model [5], the largest-cluster-control model [6], and the half-restricted random graph model [7,8]. For further models, see Ref. [9]. Owing to the research on first-order PTs, several types of underlying mechanisms for first-order PTs were uncovered: PTs induced by cascading failures such as k -core percolation [10] and on multiplex networks [11]; PTs on hyperbolic lattices [12]; and PTs induced by a rare event [13]. These examples all involve static networks in which the system size is fixed throughout the evolution of the networks.

Many networks in the real world are growing. Examples include coauthorship networks [14,15], the World Wide Web (WWW) [16], and protein interaction networks [17–19]. In growing networks, the number of nodes increases with time.

For instance, in the coauthorship network, as a new researcher joins a research group, the network grows. Callaway *et al.* [20] introduced a simple model for such growing networks, called the growing random network (GRN) model. A node is present initially. At each time, once a new node is added to the system, a link is added with probability q between a pair of unconnected nodes chosen randomly. As q is increased, a PT occurs at the transition point q_c , beyond which a giant cluster is generated. It was revealed that the PT of the GRN model follows the infinite-order Berezinskii-Kosterlitz-Thouless (BKT) transition [17,18,20,21]. The order parameter, which is the relative giant cluster size $G(q)$, is zero for $q < q_c$, whereas it increases continuously for $q > q_c$ in the essentially singular form, $G(q) \sim \exp(-a/\sqrt{q - q_c})$, where a is a positive constant. The cluster size distribution exhibits critical behavior, i.e., $n_s(q) \sim s^{-\tau(q)}$ for $q < q_c$, where $\tau(q)$ decreases down to 3 with increasing q , and $n_s(q_c) \sim 1/s^3(\ln s)^2$ [18,21]. Accordingly, the susceptibility, i.e., the mean cluster size $\langle s \rangle \equiv \sum_s s^2 n_s$, is finite on both sides of q_c . The behaviors of $G(q)$ and $\langle s \rangle$ are depicted schematically in Figs. 1(a) and 1(b).

In this Rapid Communication, we investigate how the infinite-order PT in growing networks is changed by a GS rule. Suppression dynamics may arise naturally in growing networks in the real world. For instance, in a coauthorship

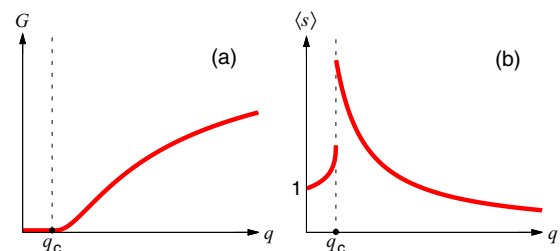


FIG. 1. Schematic plots of (a) the order parameter G and (b) the susceptibility $\langle s \rangle$ vs q for the GRN.

*sonswoo@hanyang.ac.kr

†bkahng@snu.ac.kr

network [15], as a research group becomes larger, it can become functionally inefficient; thus, new students are less likely to join such a huge group, and its growth is suppressed. To achieve our goal, we modify the GRN model by including a GS rule, as follows. Initially, a system contain a single node. At each time, a new node is added to the system. Thus, the total number of nodes at time t becomes $N(t) = t + 1$. To add a link, we select two nodes: a node from a set of the smallest clusters, denoted as R , and another node from among all the nodes of size N . They are connected with probability p . Because nodes belonging to the smallest clusters have two opportunities to be linked, whereas nodes in the remaining large clusters have a single opportunity, the growth of large clusters is suppressed. The dynamic rule becomes global in the process of sorting out the portion of the smallest clusters

among all the cluster sizes at each time. The set R contains gN nodes, whereas the complementary set R^c contains the remaining $(1 - g)N$ nodes. Further, $g \in [0, 1]$ is a parameter that controls the size of R . This model is called the restricted growing random network (r -GRN) model hereafter. The detailed rule is presented schematically in Fig. 2 and described in the caption.

We use the rate equation approach for analytic solutions and perform numerical simulations. Let us define the cluster number density $n_s(p, t)$ for a given p at time step t as the number of clusters of size s divided by the total number of nodes $N(t)$ at t . One can write the rate equations according to the cluster size s comparing to the largest cluster size in R , denoted as S_R , for the cluster size distribution $N(t)n_s$ as follows:

$$\frac{d[N(t)n_s]}{dt} = p \left[\sum_{i,j=1}^{\infty} \frac{in_i jn_j}{g} \delta_{i+j,s} - \left(1 + \frac{1}{g}\right) sn_s \right] + \delta_{1s} \quad \text{for } s < S_R, \quad (1)$$

$$\frac{d[N(t)n_s]}{dt} = p \left[\sum_{i,j=1}^{\infty} \frac{in_i jn_j}{g} \delta_{i+j,s} - sn_s - \left(1 - \sum_{k=1}^{S_R-1} \frac{kn_k}{g}\right) \right] + \delta_{1s} \quad \text{for } s = S_R, \quad (2)$$

$$\frac{d[N(t)n_s]}{dt} = p \left[\sum_{j=1}^{\infty} \sum_{i=1}^{S_R-1} \delta_{i+j,s} jn_j \frac{in_i}{g} + \sum_{j=1}^{\infty} \delta_{S_R+j,s} jn_j \left(1 - \sum_{i=1}^{S_R-1} \frac{in_i}{g}\right) - sn_s \right] \quad \text{for } s > S_R. \quad (3)$$

The first gain term on the right-hand side of Eq. (1) comes from the merging process of two clusters of size i and j . One node is randomly selected from the set R , and the other is selected from all the nodes. The second loss term comes from the merging process of one cluster of size s and another cluster of any size. The last term, with the Kronecker delta, is contributed by an incoming isolated node at each time step. Note that when $s = S_R$, the loss term needs to take into account the fact that some clusters of size S_R can belong to the set R and others with the same size can belong to the complementary set R^c . Thus, the second loss term appears in the form $p(1 - \sum_{k=1}^{S_R-1} \frac{kn_k}{g})$. When $s > S_R$, the loss term becomes simple because cluster loss occurs only when one node is selected from all the nodes. However, one needs to count the gain term carefully when one node is selected from a cluster of size S_R from the set R . We remark that to obtain the above derivation, we ignored the case in which two nodes are chosen from the same cluster. The reason is that this case contributes to the rate equations at a high order, $O(1/N^2)$. We confirm the validity of this approximation by comparing the solution of the rate equation with the result of numerical simulation later.

In the steady state, one may regard $S_R(p, t)$ and $n_s(p, t)$ as being time independent. Then the left-hand side of Eqs. (1)–(3) becomes $n_s(p)$ because $N(t) = t + 1$, and the rate equations are rewritten as follows:

$$n_s = p \left[\sum_{i,j=1}^{\infty} \frac{in_i jn_j}{g} \delta_{i+j,s} - \left(1 + \frac{1}{g}\right) sn_s \right] + \delta_{1s} \quad \text{for } s < S_R, \quad (4)$$

$$n_s = p \left[\sum_{i,j=1}^{\infty} \frac{in_i jn_j}{g} \delta_{i+j,s} - sn_s - \left(1 - \sum_{k=1}^{S_R-1} \frac{kn_k}{g}\right) \right] + \delta_{1s} \quad \text{for } s = S_R, \quad (5)$$

$$n_s = p \left[\sum_{j=1}^{\infty} \sum_{i=1}^{S_R-1} \delta_{i+j,s} jn_j \frac{in_i}{g} + \sum_{j=1}^{\infty} \delta_{S_R+j,s} jn_j \left(1 - \sum_{i=1}^{S_R-1} \frac{in_i}{g}\right) - sn_s \right] \quad \text{for } s > S_R. \quad (6)$$

The behaviors of the order parameter and mean cluster size obtained from analytic solutions and numerical simulations are shown in Fig. 3. The cluster size distributions in the three regimes are shown in Fig. 4. We find the following phase transition properties. There exist two transition points p_b and p_c ($p_b < p_c$). The giant cluster size per node is zero asymptotically for $p < p_c$, jumps at p_c , and is finite

for $p > p_c$. The size distribution of finite clusters n_s decays in a power-law manner without any cutoff as $n_s \sim s^{-\tau(p)}$ for $p < p_c$. However, it decays exponentially for $p > p_c$. Interestingly, the exponent $\tau(p)$ decreases as p is increased. $\tau(p) > 3$ for $p < p_b$, and $2 < \tau(p) < 3$ in $p_b < p < p_c$. The susceptibility, i.e., the mean cluster size $\sum s^2 n_s$, is finite and diverges in the former and latter regions, respectively.

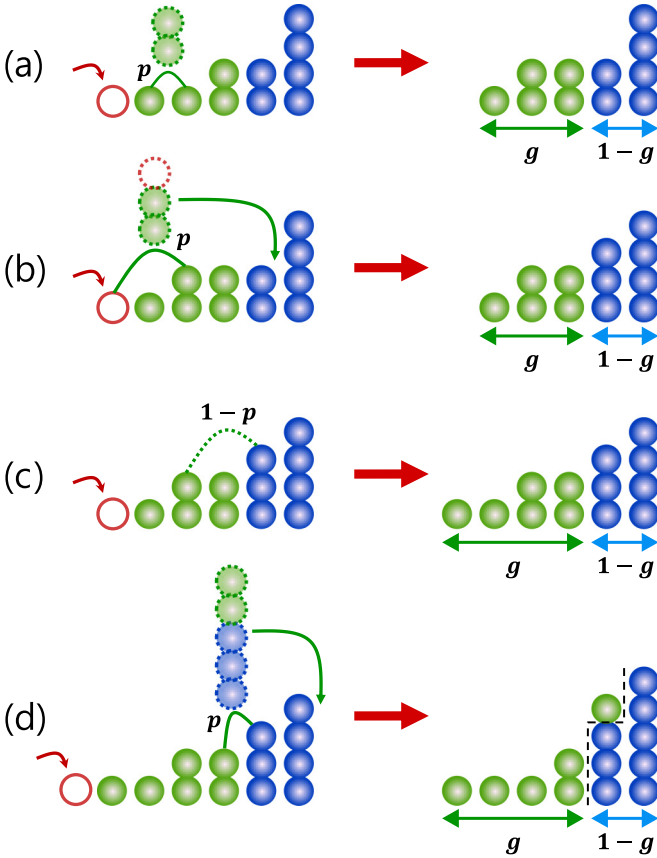


FIG. 2. Schematic illustration of the r -GRN model. Nodes (represented by balls) in set R are dark green, whereas those in R^c are blue. Each column represents a cluster. We start with the system at time $t = 9$, which contains five clusters of sizes (1, 1, 2, 2, 4) displayed from the second column on the left to the right in (a). Thus, $N(9) = 10$. Here, the control parameter g is taken as $g = 0.4$; thus, $\lceil gN \rceil = 4$. The sets R and R^c contain four (dark green) and six (blue) nodes, respectively. (a) At time $t = 10$, the leftmost red open node is newly added. $N(t) = 11$, and $\lceil gN \rceil = 5$. Next, two nodes, say, those belonging to the first and second dark green clusters of sizes (1, 1), are selected, and they are merged with probability p , making a cluster of size two. The largest cluster size in R , denoted as S_R , remains two. (b) At time $t = 11$, again a new node is added (the leftmost open red ball). The new node is selected and merges into the second cluster in R , generating a cluster of size three. Because $N(11) = 12$, $\lceil gN \rceil = 5$. The merged cluster of size three moves to R^c , whereas the cluster of size two in R^c moves to R . (c) At time $t = 12$, a new node is added. $N(12) = 13$, and $\lceil gN \rceil = 6$. Two nodes are selected, but they are not connected with probability $1 - p$. (d) At time $t = 13$, a new node is added. $N(13) = 14$, and $\lceil gN \rceil = 6$. The fifth cluster from the left in R and the first cluster in R^c merge and generate a cluster of size five that belongs to R^c . The cluster of size four then lies on the border between the two sets. In this case, one node belongs to R , and the other three belong to R^c . S_R is reset to four.

Therefore, the properties of an infinite-order transition, a second-order transition, and a first-order transition appear in the regions $p < p_b$, $p_b < p < p_c$, and $p_c < p$, respectively.

We note that $\tau = 3$ at p_b in the r -GRN model implies that p_b corresponds to q_c in the GRN model. Thus, the mean cluster size is finite up to p_b . Under the GS effect, the transition

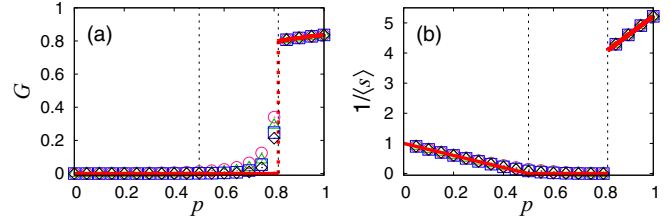


FIG. 3. Plot of (a) G and (b) $1/\langle s \rangle$ as a function of p for the r -GRN model with $g = 0.2$. Symbols represent the numerical simulation results for system sizes $N = 10^4$ (\circ), 10^5 (\triangle), 10^6 (\square), and 10^7 (\diamond). Each data point was averaged over 10^3 configurations. The solid (red) lines are analytic results. The two vertical dotted lines represent p_b and p_c .

point is delayed, and $\tau(p)$ decreases further to two at p_c , which is the extreme case. On the other hand, if the cluster size distribution follows a power law without any exponential cutoff, the largest cluster size scales with the current total number of nodes $N(t)$ in the steady state as $s_{\max} \sim N^{1/(\tau-1)}$. When τ decreases to two, the largest cluster grows to the extent of the system size in the steady state. Even though the largest cluster size increases continuously as p is increased to p_c in finite systems, the giant cluster size is still subextensive to $N(t)$ for $p < p_c$, and it becomes extensive to $N(t)$ at $p = p_c$. Thus, a discontinuous transition occurs at p_c in the thermodynamic limit. Therefore, there exist three regimes, in which the infinite-order, second-order, and first-order transition behaviors occur successively as p is increased.

The exponent τ also depends on the model parameter g , which is related to the suppression strength. gN nodes in the small-cluster group have twice the opportunity to be linked, whereas the remaining $(1 - g)N$ nodes have one opportunity. When $g = 1$, the r -GRN model reduces to the GRN model without any suppression effect; however, in the limit $g \rightarrow 0$, only isolated nodes have twice the opportunity, whereas the other nodes have only one opportunity. Thus, the suppression strength becomes large as g decreases. Figure 5 shows the phase diagram of the three phases as a function of the parameters g and p . Indeed, the phase boundaries determined by the criteria $\tau = 3$ and $\tau = 2$ depend on g .

To explore the rough dependence of τ on p , we consider a simple case in the limit $g \rightarrow 1/N$. In this case, cluster merging dynamics occur only between isolated nodes and another cluster of any size. Then, the recurrence relation for n_s in the steady state is written as

$$\frac{d[N(t)n_1]}{dt} = -p(n_1 + 1) + 1, \quad (7)$$

$$\frac{d[N(t)n_s]}{dt} = p[(s - 1)n_{s-1} - sn_s] \quad \text{for } s > 1. \quad (8)$$

In the steady state, one may regard $n_s(p, t)$ as being time independent. Then the left-hand side of Eqs. (7) and (8) becomes $n_s(p)$ because $N(t) = t + 1$, and the rate equations are rewritten as follows:

$$n_1 = -p(n_1 + 1) + 1, \quad (9)$$

$$n_s = p[(s - 1)n_{s-1} - sn_s] \quad \text{for } s > 1. \quad (10)$$

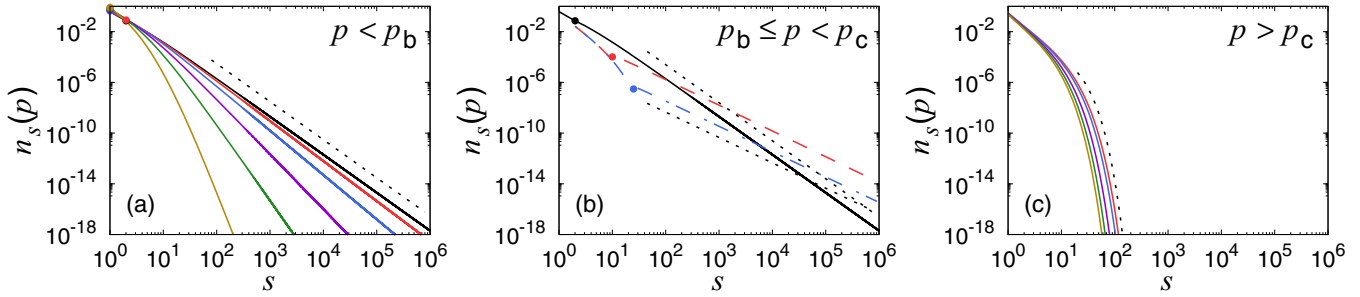


FIG. 4. Cluster size distribution $n_s(p)$ as a function of s in different p regions. Three cases of $n_s(p)$ are distinguished for $g = 0.4$. (a) For $p < p_b$, $n_s(p)$ asymptotically follows the power law $\sim s^{-\tau(p)}$ with $\tau > 3$. The slope of the dotted guide line is -3 . Solid lines are obtained for $p = 0.472\,576 \approx p_b, 0.45, 0.4, 0.3, 0.2$, and 0.1 from right to left. (b) For $p_b \leq p < p_c$, in the small-cluster-size region, $n_s(p)$ decays exponentially and then exhibits power-law behavior with $2 < \tau \leq 3$. Solid (black), dashed (red), and dashed-dotted (blue) lines represent $n_s(p)$ for $p = 0.472\,576, 0.657$, and $0.659\,45$, respectively. Two dotted lines are guide lines with slopes of -2 and -3 . (c) For $p \geq p_c$, $n_s(p)$ for finite clusters shows exponentially decaying distributions. Solid curves represent $p = 0.6596, 0.7, 0.8, 0.9$, and 1.0 from right to left. The dotted curve is an exponentially decaying guide curve.

Therefore,

$$n_s(p) = \frac{\Gamma(s)\Gamma(\frac{1}{p} + 2)}{\Gamma(s + \frac{1}{p} + 1)} n_1(p) \sim s^{-\left(\frac{1}{p} + 1\right)}. \quad (11)$$

The exponent $\tau(p) = 1 + 1/p$ is independent of g . τ becomes two when $p = 1$ as $g \rightarrow 0$. These features can be seen in Fig. 5.

The BKT transition was found originally in the two-dimensional XY model in thermal systems [22–27]. The underlying mechanism of the thermal BKT transition differs from that of the PT in growing networks, but they share some common properties. The singular part of the free energy of the XY model behaves as $f(t) \sim \exp(-bt^{-1/2})$ with a positive constant b for the reduced temperature $t = (T - T_c)/T_c > 0$. The PT order parameter $G(p)$ of the GRN model behaves similarly for $p > p_c$.

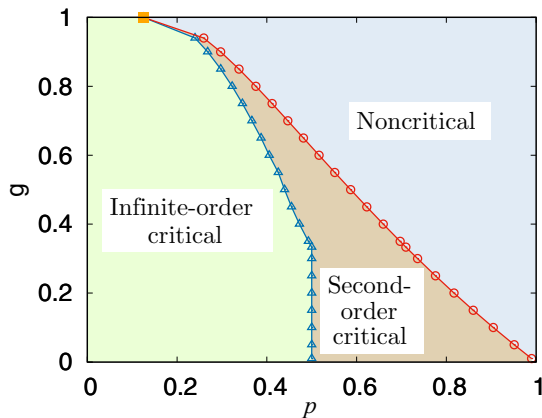


FIG. 5. Phase diagram of the r -GRN model. Two transition points, p_b (Δ) and p_c (\circ), are determined for various g . $n_s(p, g)$ decays following a power law with $\tau(p) > 3$ in the infinite-order critical region and $2 < \tau(p) < 3$ in the second-order critical region. Thus, the mean cluster size is finite and diverges in those regions, respectively. As g approaches one, the two transition points are closer and converge to the critical point of an infinite-order transition, represented by \blacksquare .

The correlation function decays in a power-law manner as $\Gamma(r) \sim r^{-\eta(T)}$ for $t < 0$ in a thermal system, where the exponent $\eta(T) \sim T$ varies continuously depending on the temperature T . This continuously varying exponent $\eta(T)$ corresponds to the continuously varying exponent $\tau(p) - 1$ in percolation, because the susceptibility is obtained from $\chi \sim \int d^2r \Gamma(r)$ in the thermal system and $\sum s^2 n_s$ in percolation. The susceptibility diverges for $\eta < 2$ in thermal systems, which corresponds to the behavior for $\tau < 3$ in the percolation system. The correlation length $\xi(t) = \infty$ for $t < 0$ in thermal systems. The characteristic cluster size $s^* = \infty$ for $p < p_c$ in percolation. On the other hand, for the GRN model proposed by Callaway *et al.* [20], $\tau > 3$ for $p \leq p_c^*$, with a logarithmic correction at p_c^* [18,21], and thus the susceptibility is finite at $p = p_c^*$, where p_c^* is the percolation threshold of the GRN model. However, for the r -GRN model, it diverges in the region $p_b \leq p \leq p_c$, because $2 \leq \tau \leq 3$ in that region. Thus, χ diverges at p_c . This result implies that the r -GRN model behaves more as the BKT transition in the thermal system than the GRN model does.

The BKT transition can occur even in static networks, for instance, the hierarchical networks with short-range and long-range connections [12,28]. It would be interesting to check whether the diverse phases and phase transitions we obtained occur in that static network when the GS rule is applied. Pattern formation by topological defects in liquid crystals has recently drawn considerable attention [29,30]. Various patterns generated in that system are essentially governed by the BKT transition. It would be nontrivial and interesting to note how those patterns can be changed when the system is subjected to a certain GS dynamics.

The reduction of the exponent $\tau = 2$ at p_c from $\tau = 3$ by the GS effect implies that the system exhibits the maximum diversity of cluster sizes. In complex systems, diversity is a crucial factor for sustaining systems in diverse fields, for example, financial-economic systems [31] and evolving biosystems [32]. Thus, the idea of the GS may be helpful for establishing affirmative action policies in financial systems or other evolving systems. Moreover, this idea could be applied to diverse nonequilibrium-phenomenon-based models such as epidemic models [33], voter models [34], and so on.

In summary, we investigated how the BKT infinite-order PT in growing networks responds to a globally suppressive environment against the growth of large clusters. The transition point is delayed, and the critical region of the BKT transition is extended. In the extended region, the fluctuations of finite clusters diverge, as we often observe in second-order transitions, but the giant cluster does not form. At the transition point, the order parameter jumps from zero to a finite value, so a first-order transition occurs. Accordingly,

those anomalous transition behaviors occur beyond the BKT transition in growing networks.

This research was supported by the National Research Foundation of Korea (NRF) through Grants No. NRF-2014R1A3A2069005 (B.K.) and No. NRF-2017R1D1A1B03032864 (S.W.S.), and a TJ Park Science Fellowship from the POSCO TJ Park Foundation (S.W.S.).

-
- [1] D. J. Thouless, *Phys. Rev.* **187**, 732 (1969).
 [2] P. Grassberger, *J. Stat. Mech.* (2013) P04004.
 [3] D. Achlioptas, R. M. D'Souza, and J. Spencer, *Science* **323**, 1453 (2009).
 [4] O. Riordan and L. Warnke, *Science* **333**, 322 (2011).
 [5] Y. S. Cho, S. Hwang, H. J. Herrmann, and B. Kahng, *Science* **339**, 1185 (2013).
 [6] N. A. M. Araújo and H. J. Herrmann, *Phys. Rev. Lett.* **105**, 035701 (2010).
 [7] K. Panagiotou, R. Sphöel, A. Steger, and H. Thomas, *Electron. Notes Discrete Math.* **38**, 699 (2011).
 [8] Y. S. Cho, J. S. Lee, H. J. Herrmann, and B. Kahng, *Phys. Rev. Lett.* **116**, 025701 (2016).
 [9] R. M. D'Souza and J. Nagler, *Nat. Phys.* **11**, 531 (2015).
 [10] G. J. Baxter, S. N. Dorogovtsev, K. E. Lee, J. F. F. Mendes, and A. V. Goltsev, *Phys. Rev. X* **5**, 031017 (2015).
 [11] S. V. Buldyrev, R. Parshani, G. Paul, H. E. Stanley, and S. Havlin, *Nature (London)* **464**, 1025 (2010).
 [12] S. Boettcher, V. Singh, and M. R. Ziff, *Nat. Commun.* **3**, 787 (2012).
 [13] G. Bianconi, *Phys. Rev. E* **97**, 022314 (2018).
 [14] M. E. Newman, *Proc. Natl. Acad. Sci. USA* **101**, 5200 (2004).
 [15] D. Lee, K.-I. Goh, B. Kahng, and D. Kim, *Phys. Rev. E* **82**, 026112 (2010).
 [16] J. Leskovec, J. Kleinberg, and C. Faloutsos, *ACM Trans. Knowl. Disc. Data* **1**, 2 (2007).
 [17] R. V. Solé, R. Pastor-Satorras, E. D. Smith, and T. Kepler, *Adv. Complex Syst.* **05**, 43 (2002).
 [18] J. Kim, P. L. Krapivsky, B. Kahng, and S. Redner, *Phys. Rev. E* **66**, 055101 (2002).
 [19] A. Vázquez, A. Flammini, A. Maritan, and A. Vespignani, *ComplexUs* **1**, 38 (2003).
 [20] D. S. Callaway, J. E. Hopcroft, J. M. Kleinberg, M. E. J. Newman, and S. H. Strogatz, *Phys. Rev. E* **64**, 041902 (2001).
 [21] S. N. Dorogovtsev, J. F. F. Mendes, and A. N. Samukhin, *Phys. Rev. E* **64**, 066110 (2001).
 [22] V. L. Berezinskii, *Sov. Phys. JETP* **32**, 493 (1971).
 [23] V. L. Berezinskii, *Sov. Phys. JETP* **34**, 610 (1972).
 [24] J. M. Kosterlitz and D. J. Thouless, *J. Phys. C* **5**, L124 (1972).
 [25] J. M. Kosterlitz and D. J. Thouless, *J. Phys. C* **6**, 1181 (1973).
 [26] J. M. Kosterlitz, *J. Phys. C* **7**, 1046 (1974).
 [27] J. M. Kosterlitz, *Rev. Mod. Phys.* **89**, 040501 (2017).
 [28] A. N. Berker, M. Hinczewski, and R. R. Netz, *Phys. Rev. E* **80**, 041118 (2009).
 [29] M. C. Marchetti, J. F. Joanny, S. Ramaswamy, T. B. Liverpool, J. Prost, Madan Rao, and R. Aditi Simha, *Rev. Mod. Phys.* **85**, 1143 (2013).
 [30] X. Tang and J. Selinger, *Soft Matter* **13**, 5481 (2017).
 [31] X. Gabaix, *Annu. Rev. Econ.* **1**, 255 (2009).
 [32] E. M. Rauch and Y. Bar-Yam, *Nature (London)* **431**, 449 (2004).
 [33] R. Pastor-Satorras, C. Castellano, P. van Mieghem, and A. Vespignani, *Rev. Mod. Phys.* **87**, 925 (2015).
 [34] C. Castellano, S. Fortunato, and V. Loreto, *Rev. Mod. Phys.* **81**, 591 (2009).